

Kent Academic Repository

Full text document (pdf)

Citation for published version

Posada-Roman, Julio E. and Jackson, David A. and Garcia-Souto, Jose A. (2016) Variable configuration fiber optic laser doppler vibrometer system. *Photonic Sensors*, 6 (2). pp. 97-106. ISSN 1674-9251.

DOI

<https://doi.org/10.1007/s13320-016-0293-0>

Link to record in KAR

<http://kar.kent.ac.uk/61954/>

Document Version

Publisher pdf

Copyright & reuse

Content in the Kent Academic Repository is made available for research purposes. Unless otherwise stated all content is protected by copyright and in the absence of an open licence (eg Creative Commons), permissions for further reuse of content should be sought from the publisher, author or other copyright holder.

Versions of research

The version in the Kent Academic Repository may differ from the final published version.

Users are advised to check <http://kar.kent.ac.uk> for the status of the paper. **Users should always cite the published version of record.**

Enquiries

For any further enquiries regarding the licence status of this document, please contact:

researchsupport@kent.ac.uk

If you believe this document infringes copyright then please contact the KAR admin team with the take-down information provided at <http://kar.kent.ac.uk/contact.html>

Variable Configuration Fiber Optic Laser Doppler Vibrometer System

Julio E. POSADA-ROMAN¹, David A. JACKSON^{2*}, and Jose A. GARCIA-SOUTO¹

¹*Department of Electronics Technology, GOTL University Carlos III de Madrid, Butarque 15, 28911, Leganés, Madrid, Spain*

²*Applied Optics Group, School of Physical Sciences, University of Canterbury, Kent, CT2 7NH, UK*

*Corresponding author: David A. JACKSON E-mail: d.a.jackson@kent.ac.uk

Abstract: A multichannel heterodyne fiber optic vibrometer is demonstrated which can be operated at ranges in excess of 50 m. The system is designed to measure periodic signals, impacts, rotation, 3D strain, and vibration mapping. The displacement resolution of each channel exceeds 1 nm. The outputs from all channels are simultaneous, and the number of channels can be increased by using optical switches.

Keywords: Laser Doppler; vibration; digital processing; nanometer resolution; multiplexing; optical fiber

Citation: Julio E. POSADA-ROMAN, David A. JACKSON, and Jose A. GARCIA-SOUTO, "Variable Configuration Fiber Optic Laser Doppler Vibrometer System," *Photonic Sensors*, 2016, 6(2): 97–106.

1. Introduction

Laser Doppler vibrometers (LDV) based on a Mach-Zehnder interferometer (MZI) incorporating an external air path with a Bragg cell frequency modulator have been available for several decades. Displacement resolution of $\sim 1 \times 10^{-9}$ m has been achieved with these devices typically illuminated with relatively low power single frequency He-Ne laser. One of the major factors responsible for the high spatial resolution is the very low phase noise and nearly perfect Gaussian beam exhibited by these lasers. A problem with conventional LDVs is that a direct line of sight between the instrument and the target is required making it difficult to make measurements in confined or restricted areas. It is also not possible to make measurements at more than one location at a time with these LDVs. To overcome these problems, we have designed and

implemented a multichannel fiber optic based laser Doppler heterodyne vibrometer (FLDV) which can be operated at ranges from \sim cm to more than 50 m. The vibrometer can be used to measure signals such as displacement impacts, rotation, strain and torsional vibrations. The displacement resolution of each channel exceeds 1 nm at frequencies up to 100 kHz (limited by the shakers available). The outputs from all channels are simultaneous; the number of channels can be increased using optical switches.

2. Conventional laser Doppler vibrometer

A conventional LDV is shown in Fig. 1. Light from a single frequency He-Ne laser is injected into a cube beam splitter (CBS1) where it is amplitude divided. One of the output laser beams propagates to CBS3 and is focused by the lens onto the target. The back reflected beam from the target is transferred to CBS4 via CBS3. The other output beam from CBS1

Received: 11 December 2015 / Revised: 4 March 2016

© The Author(s) 2016. This article is published with open access at Springerlink.com

DOI: 10.1007/s13320-016-0293-0

Article type: Regular

is reflected at CBS2 transferring it to the Bragg cell where it undergoes a frequency shift of typically 40 MHz. These beams interfere in CBS4 generating an optical interference signal at 40 MHz which is transposed to an electrical signal by the photodiodes. The outputs from the detectors can be combined differentially to minimize noise. When the target is subject to vibration, side bands are generated symmetrically around 40 MHz which are described by Bessel functions of the first kind. This signal is processed electronically to recover the frequency and amplitude of vibration of the target.

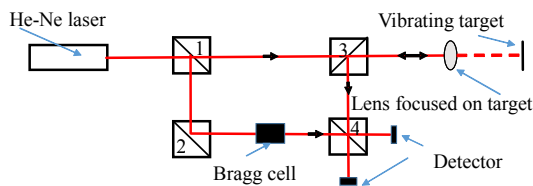


Fig. 1 Conventional laser Doppler vibrometer.

3. Fiber optic laser Doppler vibrometer

Figure 2 shows an implementation of an optical FLDV. Light from a single frequency 1.5 micron laser diode with low phase and intensity noise is pigtailed to low loss single mode optical fiber producing a Gaussian beam at the distal end of the fiber. This guided beam is injected into the first 3 dB coupler as shown in Fig. 2. One output from the coupler is connected to a circulator which sends the fiber guided light to a target via a variable focus collimator generating a tightly focused Gaussian disc. The back reflected light from the target is coupled back into the fiber and hence the circulator, and transferred to the input of the second coupler. The other optical output from the first coupler is frequency shifted by the 40 MHz Bragg cell (as discussed above) and injected into the other input port of the second 3 dB coupler. Optical interference occurs at this coupler and is detected by a low noise 125 MHz optical detector [1]. Additionally, an inline variable attenuator in the MZI arm containing the Bragg cell is used to prevent saturation of the detector.

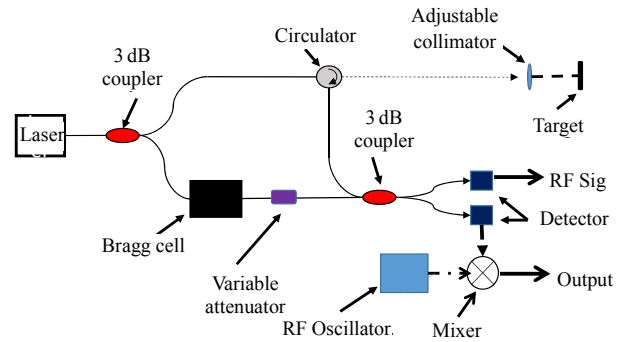


Fig. 2 Fiber laser Doppler vibrometer including a mixer to down shift recovered signal.

Optical fiber components can be fused together with extremely low optical loss; in addition, no optical alignment is required except the collimator with the target. As the FLDV is a complex MZI, we need to consider the impact on the fringe visibility of large optical path differences (OPDs). Ideally, the optical path length (OPL) of the sensing arm should equal the OPL of the reference arm. This would be very difficult to achieve in practice, however this requirement can be ameliorated to a large extent as the laser source used has an extremely narrow linewidth of less than 1 MHz. This corresponds to a coherence length of ~ 200 m, implying that it is unnecessary to closely match the OPDs of the sensor and reference paths.

As discussed above, the spectrum of the light backscattered from a vibrating target will generate a phase modulated signal at 40 MHz, which is described by Bessel functions [3]. The spectrum will be much more complicated for random modulation of the target. The signal can be analyzed with an electronic spectrum analyzer or a “phase locked loop” which can give valuable but limited information. A digital processor offers the best solution as it is able to recover the amplitude, frequency, and phase of the signal with higher accuracy. Rather than directly processing the signal at 40 MHz (Fig. 3(a)), it can be transposed to a lower frequency using an electronic mixer and a second high frequency oscillator at 39.9 MHz as shown in Fig. 2. An example of the resultant down shifted

carrier is shown in Fig. 3(b).

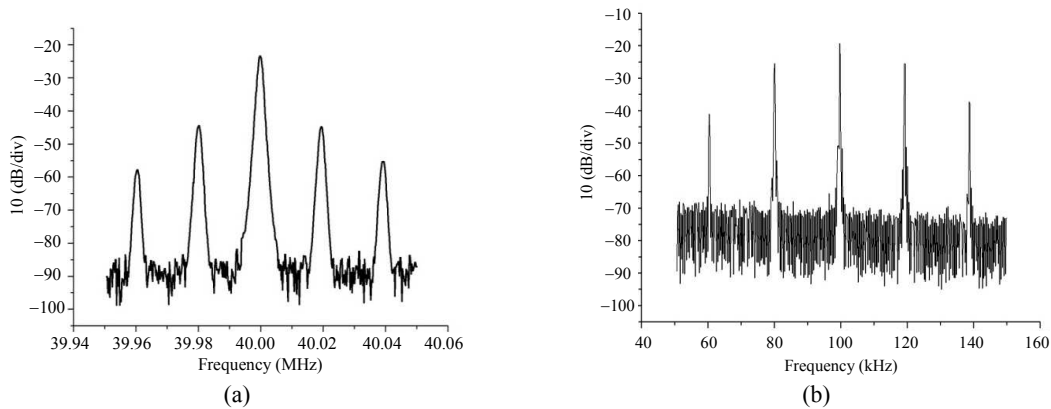


Fig. 3 Spectra of the optical carrier: (a) carrier at 40 MHz modulated at a frequency of 20 kHz and (b) the carrier frequency is 100kHz modulated at 20kHz.

4. Digital high speed processing system for heterodyne FLDV and calibration

4.1 Digital demodulator

Figure 4 shows the basic scheme proposed for the heterodyne FLDV signal recovery. The DAQ and signal processing implement an I/Q phase demodulation instead of a frequency demodulation [2]. It is completely digital and is implemented in LabVIEW. This reduces the size of the system and

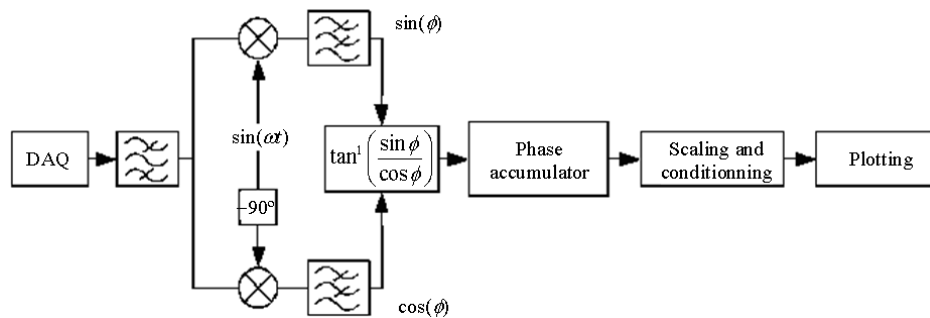


Fig. 4 Schematic of digital processing.

4.2 Performance of the heterodyne FLDV

Initial studies were performed to assess the performance of the 4-channel heterodyne FLDV. A simple method that exploits the Bessel function of first kind can be used for this propose [3]. It is based on the measurement of the ratio of

$$J_0(m) = J_1(m) \quad (1)$$

$$m = 2kx \quad (2)$$

facilitates the implementation of a multichannel FLDV due to the software scalability.

By means of the I/Q demodulation, the sine and cosine of the carrier are obtained, and the phase angle is recovered using the arctangent function. The heterodyne detection together with the digital demodulation provides a wider measurement range because a digital phase accumulator can be implemented (Fig. 4) for fringe counting which extends the measurement range further than 2π radians.

where $J_n(m)$ is a Bessel function of the first kind order n and modulation index m , $k=2\pi/\lambda$, x is the displacement, and λ is the wavelength of the laser. A spectrum analyzer was used to monitor the carrier, and the harmonics produced by the modulation of a shaker used as a vibrating target for the calibration. The amplitude of the vibration was set to obtain the particular condition when $J_0 = J_1$. This calibration point corresponds to a modulation index $m = 2.4$ and

can be used in (2) in order to find the magnitude of the target displacement. The carrier signal was observed with the spectrum analyzer for a stationary target (without vibration), when it is vibrating at 20 kHz with an amplitude corresponding to the calibration point where $J_0 = J_1$ are shown in Figs. 5(a) and 5(b), respectively.

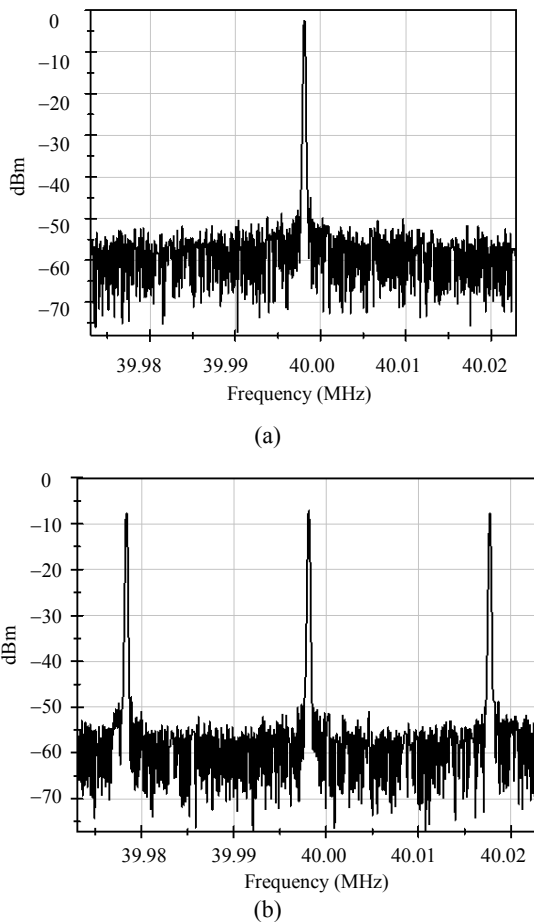


Fig. 5 Spectra recovered from a vibrating target: (a) spectrum of the un-modulated carrier and (b) spectrum of the carrier modulated at $J_0 = J_1$ (RBW=100 Hz).

The data shown in Fig. 6 are the typical amplitude noise (in microns) observed at the output

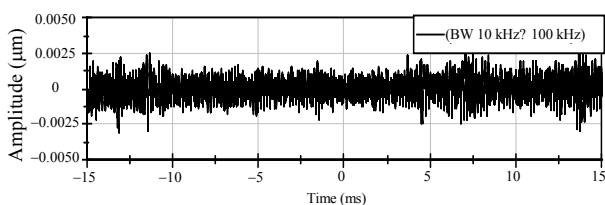


Fig. 6 Typical amplitude noise observed in a bandwidth of 90 kHz when the system is illuminated with a single frequency distributed feedback laser (DFB).

of the digital I/Q demodulator when the target is stationary. The amplitude of the noise measured in a bandwidth of 90 kHz was 0.7 nm (RMS), i.e. $2 \text{ pm}/\sqrt{\text{Hz}}$.

5. Multi-channel FLDV system

In this section, we consider optical fiber topologies for multichannel probes which allow simultaneous measurement for all channels [4–6]. The description of the mode of operation is for 4 channels but 8 channels or more are possible dependent on the source power available. Optical amplifiers can be used to increase the number of channels which could be deployed, providing the coherence of the illuminating laser is not affected. In addition, optical switches can be used at other channels as described above.

The fiber topology of the 4-channel system is based on the 4-channel multiplexing unit shown in Fig. 7. The input beam from the single frequency laser diode is initially divided by a 3 dB coupler. One of the outputs is transferred to a 4-channel fiber optic power divider. Each of the 4 emanating fiber guided beams propagates through separate fiber circulators and then via fiber links to adjustable fiber collimators that are focused on 4-individual targets. Light back scattered/reflected from the targets is re-injected back into the collimators and propagates to the inputs of a set of four 3 dB couplers via the third port of each circulator.

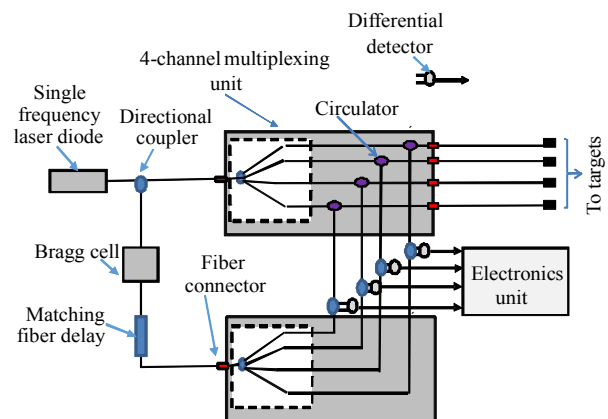


Fig. 7 Scheme of a four channel FLDV.

The other beam ejected from the 3 dB coupler via a delay and Bragg cell is divided into four guided beams by a 1×4 channel power divider. The 4 beams propagate to the 4 input ports of the set of 3 dB couplers where optical interference occurs. The four interferometric signals are detected with (differential) optical detectors and sent to the digital processing unit.

5.1 Experimental setup of vibration tests

In order to demonstrate that data could be recovered simultaneously from four sensors, targets T1 and T2 were placed on a carbon fiber plate driven by a B&K shaker shown in Fig. 8(a). The shaker was driven by a purpose-built high power amplifier. Above the target plate, there were 2 mirror mounts in which fiber collimator probes Ch1 and

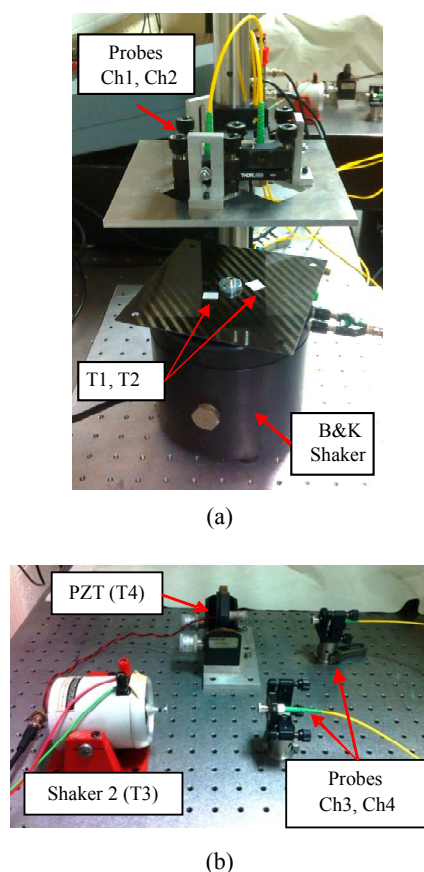


Fig. 8 Photograph in Fig. 8 shows the probes and targets: (a) Targets T1 and T2 are mounted on a carbon fiber plate with Probes Ch1 and Ch2 mounted vertically above and (b) Targets T3 and T4 are mounted vertically illuminated with horizontal beams from Probes Ch3 and Ch4, respectively.

Ch2 were mounted. The output beams were well focused on the targets. Figure 8(b) shows the arrangement of Targets T3 and T4. T3 was mounted directly on the shaft of a LING dynamics shaker, and T4 was on the end of a coaxial PZT. As in Ch1 and Ch2, the collimators were mounted in mirror mounts. The targets were chosen to simulate different target locations and vibration levels which could be encountered.

5.2 Experimental results with driven vibration sensors

Experiments were performed with the shakers being driven at different frequencies and amplitudes. Simultaneous measurements of vibration with the 4 sensors were taken in the experimental arrangement described in Section 5.1. The demodulated signals were presented as amplitude graphs in Fig. 9. Although Targets T1 and T2 were mounted on the same carbon plate, they were sufficiently far apart that there was a phase difference. The shaker of T1 and T2 was driven at 2 kHz, T3 was driven at 10 kHz, and the PZT connected to T4 was driven at 60 kHz. An optical power of ~ 2 mW provided by the DFB laser was enough to illuminate the 4-channel FLDV.

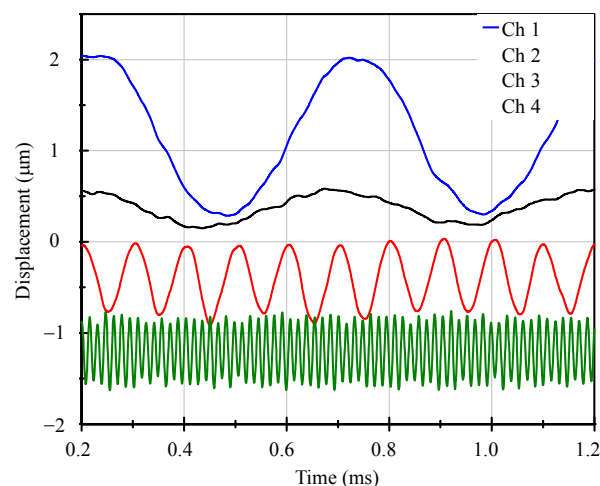


Fig. 9 Demodulated output signals from the 4 targets (the top 2 traces were generated when the B&K shaker was driven at 2 kHz with amplitudes of 0.8 microns (Ch1) and ~ 0.25 (Ch2) microns, respectively; Channel 3 (third trace from top) was generated when shaker 3 was driven at 10 kHz with amplitude of 0.4 microns and Channel 4 (bottom trace) at 60 kHz with amplitude of ~ 0.3 microns).

5.3 Large distance applications

In the multiplexing schemes described above (Fig. 7), the environments of the reference and signal arms are similar, however in field measurements, this condition cannot be maintained especially if large distances are involved. It is therefore necessary to match the operating conditions for the reference and sensor fibers.

This can be accomplished using the multiplexing scheme in Fig. 7 modified as shown in Fig. 10 such that at the output of the system the OPDs for “sensor reference pairs” are approximately equal (to better than ~ 10 cm). The reference and sensor probe transceiver leads are coupled together in a sheath to minimize the differential phase shifts induced by environmental effects in the links. The output from the sensing link is transferred to the target through a collimator. The distal face of the reference fiber has a reflective coating to ensure good fringe visibility. Typical results for a target at a 50 m measurement range vibrating at 60 kHz (amplitude of displacement is 70 nm) are shown in Figs. 11 and 12.

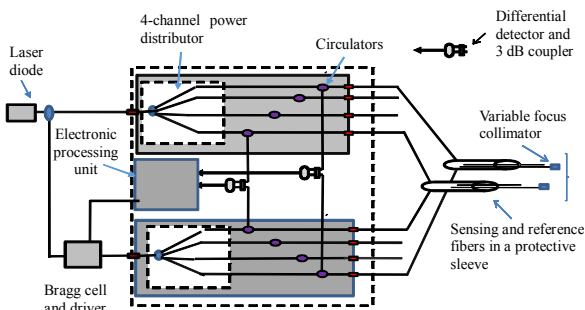


Fig. 10 Modifications of the system shown in Fig. 7 to enable large distance applications.

5.4 Increased number of channels

There are a large number of applications which require measurements to be made at more than one location where it is not essential that all the data are acquired at the same time. One low cost option is to incorporate an electrically controlled fiber bidirectional optical switch into a basic FLDV as shown in Fig. 13. Typically, the power loss for any switched channel is ~ 1.5 dB, which implies the

resolution and signal strength will only be marginal affected. A realistic number achievable by this approach is 4–8 channels. Although this is an attractive solution, the measurements at each channel are not simultaneous for example a commercial 4-channel switch takes ~ 2 ms per channel and 8 ms to make 4 sequential measurements at 4 locations. Experiments using the switch on one of the outputs from the four channels demonstrated no loss of performance.

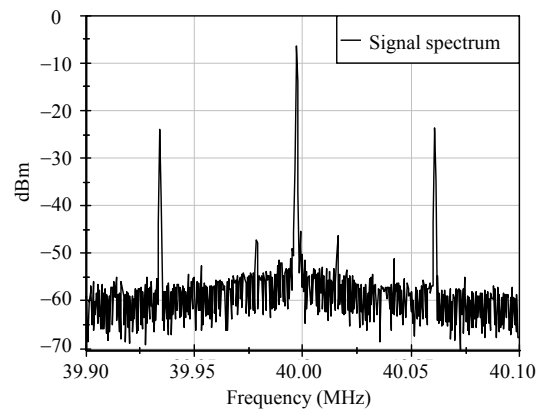


Fig. 11 Spectrum of the carrier modulated with a 60 kHz signal (PZT) measured at a range of 50 m.

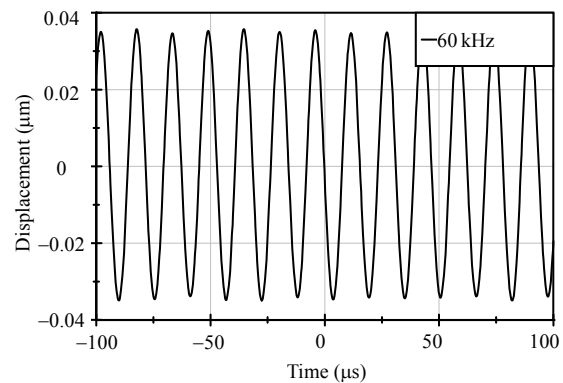


Fig. 12 Digitally demodulated signal for target at 50 m away.

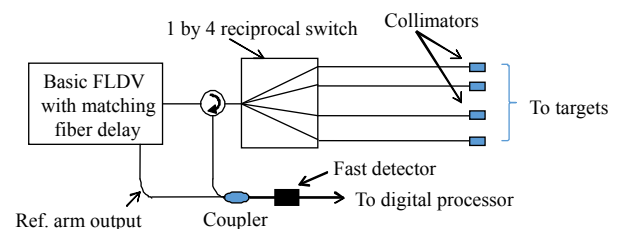


Fig. 13 Implementation of a bidirectional optical switch in the FLDV for increasing the number of channels.

6. Common path topologies

As part of this project, we explored the possibility of using a common path fiber optic topology (CPT) to form a sensor capable of making vibration measurements due to the potential simplicity of the instrumentation and low cost. A basic simple common path fiber sensor can be realized by forming an optical cavity between the distal end of a normally cleaved (transceiver fiber) and a remote target [7]. Figure 14 shows a non-contact common path sensor system. The OPD of the cavity must be less than the coherence length of the source. The input laser beam is transmitted to the target via a circulator and focused on the target and returns to the detector by the circulator. As can be seen in Fig. 14, the transceiver fiber acts as both, the reference and signal fibers for the sensor cavity. Therefore, environmental noise has a minimal impact on the system. This is especially the case for long-range measurements, as mentioned above in Section 5.3, and represents one of the main advantages of common path topology.

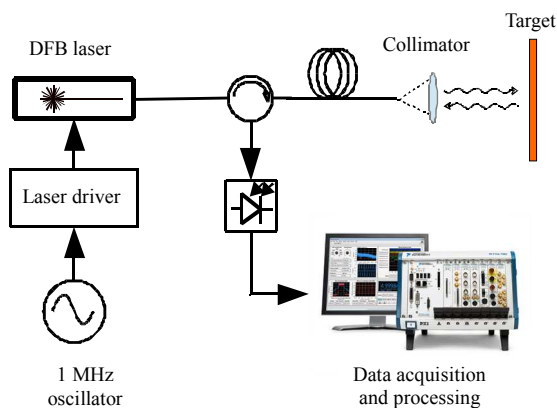


Fig. 14 Basic scheme of non-contact CPT vibrometer.

For the implementation of the CPT LDV, the cavity OPD is set at 4 cm. As in Section 6, the number of probes can be increased to 4 channels by using the multiplexing unit (Fig. 7), again a switch can also be used to increase further the number of probes.

Although the common path sensor has been used for many applications [7–9], to our knowledge there

are no reports in the literature of multiple channel common path fiber vibrometers, possibly due to problems associated with processing the data. Possible approaches for signal recovery include (a) phase generated carrier (PGC) [10], (b) channelled spectrum analysis [11], and (c) PGC with the fringe counter for every $\pm 2\pi$ phase change [2, 12]. In the work reported here, the PGC with the fringe counter approach was used. The complete system is shown in Fig. 14 and configured for testing a CPT vibrometer. A laser diode was used to illuminate the system, which was chirped over one free spectral range of the sensor cavity. This condition can be written [6] as

$$\Delta\phi_L = \frac{2\pi \cdot \Delta\nu \cdot \Delta L}{C} \quad (3)$$

where $\Delta\phi_L$ is the phase change induced in the cavity, $\Delta\nu$ is the absolute frequency shift of the laser, and ΔL is the cavity length. It can be seen from (3) that modulation of the laser optical frequency produces phase changes of the interferometric signal. PGC approach exploits this characteristic in order to generate a carrier through these induced phase changes. Typically, a laser with an extremely low phase noise combined with frequency modulation capabilities is required. By means of PGC, quadrature components of the measurement phase shift can be recovered at a specific modulation depth (when Bessel functions are $J_1=J_2$ or $J_2=J_3$, etc.). This condition of the modulation depth can be established through a closed loop that controls the amplitude of the modulating signal oscillator.

Experiments were performed using a LabVIEW controlled PXI DAQ and processing system. This can be implemented by different approaches: PGC, the fast Fourier transform, and the fringe counting, but in these experiments, the PGC approach was used. The modulation signal used to chirp the DFB laser was a sinusoid of 1 MHz frequency. Figure 15(a) shows the results of a vibration at 1 kHz measured with the CPT LDV, and Fig. 15(b) shows the Lissajous curve of the quadrature components

obtained from the PGC signal.

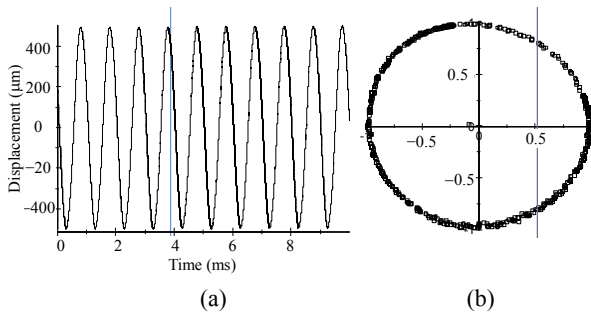


Fig. 15 Spectrum recovered with the CPT LDV and its associated Lissajous curve: (a) measurement of a target vibrating at 1 kHz and (b) Lissajous curve of the quadrature components of the signal recovered with digital processing of the PGC.

7. Measurement of rotating targets

FLDV can be used for measuring torsional vibrations, which is of interest in various applications, such as monitoring the instantaneous rotational motion of key components e.g. in car and airplane engines. Torque measurements in shafts can be also done with FLDV. This is a very interesting application for industry, but as it requires multipoint measurements the multichannel FLDV described here is ideal as it can be used to make simultaneous multipoint measurement on the shaft [13]. The multichannel FLDV in Section 5 is presented in this section for the application of rotational speed and torque measurements.

7.1 Rotational speed sensor

The geometry used for the determination of the angular rotation of a disc is shown Fig. 16, indicating the illumination point on the axis and its distance from the axis and (b) photographs of the disc and probe.

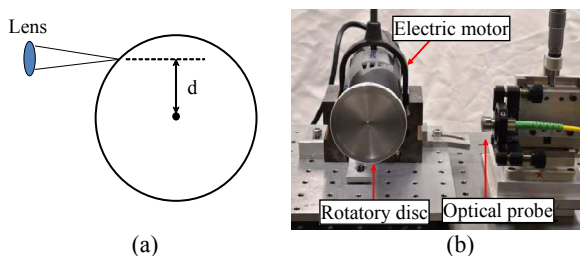
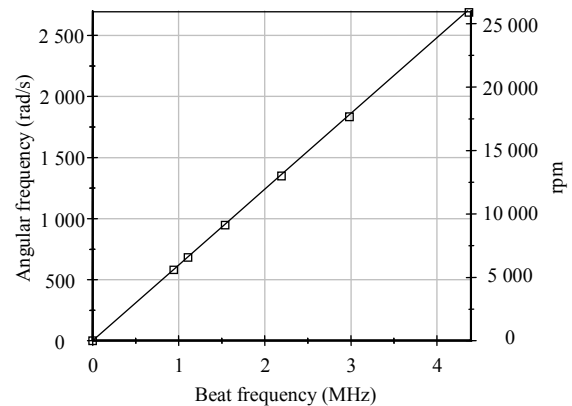
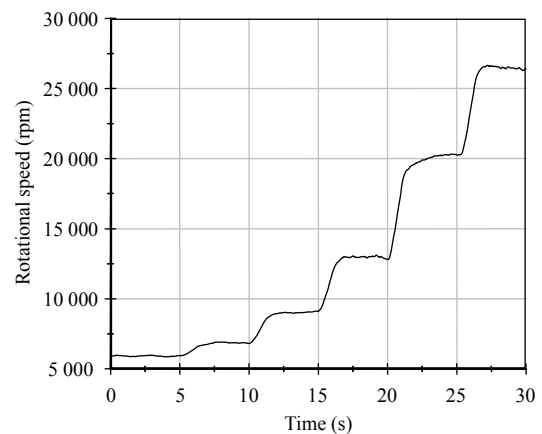


Fig. 16 Arrangement for measuring the axial rotation of a disc: (a) schematic diagram indicating the illumination point on the rim and its distance from the axis and (b) photographs of the disc and probe.

The Doppler frequency shift induced by the rotational motion is $2d\omega/\lambda$ [13], where ω is the angular frequency, d is the distance between the axis and center of the disc, and λ is the wavelength of the light. The formula is only correct if the back scattered beams are perpendicular to the axis of the disc. In this work, we only measured the angular velocity using one channel of the system. Normally, the torque was measured using 2 laser beams focused on the rim of the disc or shaft symmetrically either side of a diameter. A setup was prepared for rotational speed measurements using a rim of 6 cm in diameter with its axis connected to a high speed electric motor. The FLDV with the configuration shown in Fig. 7 was used in this experiment for the



(a)



(b)

Fig. 17 Results from rotational speed measurement: (a) angular frequency of the disc as a function of the measured beat frequency and (b) step changes in rotational speed as its driving voltage is slowly stepped in time (measurement range from 6000 rpm to 26000 rpm).

rotational speed measurements. During the experiment, the speed of the electric motor was changed in steps, and the output of the FLDV was monitored. The results of Fig. 17(a) show the angular frequency of the disc as a function of the measured Doppler frequency shift, and Fig. 17(b) shows the step changes in rotational speed as it is slowly stepped in time.

7.2 Proposed optical torque sensor

An optical torque sensor requires that the angular velocity was measured at 2 locations at a specified distance apart. To eliminate non radial movement, 2 probes would be used at each location where the focused beams were set symmetrically about the axis of the shaft. Figure 18 shows how the top 2 probes would be used to make the compensated angular velocity measurement at Location 1. Similarly, the 2 bottom probes would be used to make measurements at the 2nd location. Subtraction of data yields the differential phase and hence the dynamic torque. The optical system shown in Fig. 7 requires no modifications for dynamic torque measurements on shafts.

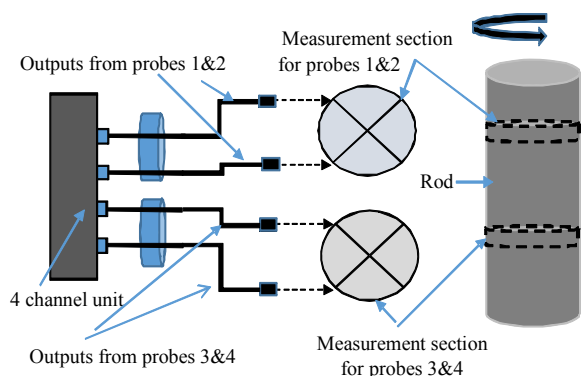


Fig. 18 Proposed torque sensor with the 4-channel power distribution unit.

8. Summary and conclusions

8.1 Multichannel fiber laser Doppler vibrometer

A 4-channel FLDV with a displacement resolution better than 1 nm at frequencies up to 60 kHz, limited by the shakers available, was

presented. The maximum frequency was set by the Bragg cell at ~40 MHz. A laser power of ~2 mW was sufficient to support the 4-channel FLDV; 8 channels – 16 channels could be supported with 4 mw – 8mw. Digital signal processing was used to recover and present the data. Absolute calibration of the FLDV was via the Bessel function ratio $J_0(m)=J_1(m)$, and other ratios could be used. An optical fiber switch was used to expand the number of channels. The design of the system based on the compact optical power transceiver unit makes it portable enabling application outside the benign laboratory environment. The system can also be used for angular velocity and torque measurements.

8.2 Common path vibrometer

An initial study of a common path vibrometer cavity indicated that it could be used to recover the dynamic motion of a target. When a target was subject to a constant amplitude sinusoidal signal, excellent optical fringes were observed allowing a fast Fourier transform (FFT) to recover the signal applied to the shaker; similarly for a multi-probe system. Excellent raw data were obtained for vibration studies in both local measurement and at large distances. A chirped laser was used to implement a PGC approach in the CPT. This enabled the recovery of the measurement using a digital quadrature demodulation.

8.3 Applications and impact tests

Applications for single channel LDV and FLDV for precision measurements were well reported in the literature. Multichannel FDLV can be used in situations where there is limited access and where many locations must be measured for example multi-valve diesel engines. The proposed topologies enhance the utility of FDLV for two major applications currently in progress. One is to study the effects of hypervelocity impacts in a light gas gun (University of Kent) that can project a single particle with velocities in excess of 10 km/s [14].

Targets are typically materials used for satellites or aerospace applications. The 4-channel FLDV could give 4 simultaneous high accuracy vibration signals generating data previously unobtainable. The second study, where common path vibrometers will be used, is related to the damage caused to high speed trains by stones sucked up from the track caused by passage of the trains.

Acknowledgment

Author J. E. Posada acknowledges a short term mobility grant from University Carlos III de Madrid to undertake research at the University of Kent, School of Physical Sciences, Canterbury, Kent.

Open Access This article is distributed under the terms of the Creative Commons Attribution 4.0 International License (<http://creativecommons.org/licenses/by/4.0/>), which permits unrestricted use, distribution, and reproduction in any medium, provided you give appropriate credit to the original author(s) and the source, provide a link to the Creative Commons license, and indicate if changes were made.

References

- [1] A. C. Lewin, A. D. Kersey, and D. A. Jackson, "Non-contact surface vibration analysis using a monomode fiber optic interferometer incorporating an open air path," *Journal of Physics E Scientific Instruments*, 1985, 18(7): 604–608.
- [2] J. E. Posada, J. A. Garcia-Souto, and J. Rubio-Serrano, "Multichannel optical-fiber heterodyne interferometer for ultrasound detection of partial discharges in power transformers," *Measurement Science & Technology*, 2013, 24(9): 94015–94023.
- [3] D. A. Jackson, J. E. Posada-Roman, and J. A. Garcia-Souto, "Calibration of laser Doppler vibrometer exploiting Bessel functions of the first kind," *Electronics Letters*, 2015, 51(14): 1100–1102.
- [4] C. Yang, M. Guo, H. Liu, K. Yan, Y. Xu, H. Miao, *et al.*, "A multi-point laser Doppler vibrometer with fiber-based configuration," *Review of Scientific Instruments*, 2013, 84(12): 121702-1–121702-6.
- [5] Y. Fu, M. Guo, and P. B. Phua, "Multipoint laser Doppler vibrometry with single detector: principles, implementations, and signal analyses," *Applied Optics*, 2011, 50(10): 1280–1288.
- [6] D. A. Jackson, "Monomode optical fiber interferometers for precision measurement," *Journal of Physics E Scientific Instruments*, 1985, 18(12): 981–1001.
- [7] M. Schulz and P. Lehmann, "Measurement of distance changes using a fibre-coupled common-path interferometer with mechanical path length modulation," *Measurement Science & Technology*, 2013, 24(24): 48–49.
- [8] T. O. H. Charrett, S. W. James, and R. P. Tatam, "Optical fibre laser velocimetry: a review," *Measurement Science & Technology*, 2012, 23(3): 32001–32032.
- [9] K. M. Tan, M. Mazilu, T. H. Chow, W. M. Lee, K. Taguchi, B. K. Ng, *et al.*, "In-fiber common-path optical coherence tomography using a conical-tip fiber," *Optics Express*, 2009, 17(4): 2375–2384.
- [10] M. J. Connelly, "Digital synthetic-heterodyne interferometric demodulation," *Journal of Optics A Pure & Applied Optics*, 2002, 4(6): S400–S405.
- [11] D. A. Jackson, "High temperature Fabry-Perot probe interrogated with tunable fibre ring laser," *Electronics Letters*, 2008, 44(15): 898–899.
- [12] J. Bush, A. Cekorich, and C. K. Kirkendall, "Multichannel interferometric demodulator," in *Proc. SPIE*, vol. 3180, pp. 19–29, 1997.
- [13] T. Y. Liu, M. Berwick, and D. A. Jackson, "Novel fibre-optic torsional vibrometers," *Review of Scientific Instruments*, 1992, 63(4): 2164–2169.
- [14] D. A. Jackson and M. J. Cole, "Fiber optic interrogation systems for hypervelocity and low velocity impact studies," *Photonic Sensors*, 2012, 2(1): 50–59.